



## Removal of erythromycin antibiotic from the aqueous media using magnetic graphene oxide nanoparticles

Parya Fathollahi<sup>a</sup>, H. Salehzadeh<sup>b</sup>, Katayon Hosseini<sup>c</sup>, K. Wantala<sup>d</sup>, H.P. Shivaraju<sup>e</sup>, D. Jenkins<sup>f</sup>, B. Shahmoradi<sup>g,h,\*</sup>

<sup>a</sup>Department of Environment, Faculty of Natural Resources, Gorgan University of Agricultural Sciences and Natural Resources, Gorgan, Iran, email: paryafathollahi@yahoo.com

<sup>b</sup>Student Research Committee, Kurdistan University of Medical Sciences, Sanandaj, Iran, email: hamzeh.salehzadeh@gmail.com

<sup>c</sup>Department of Environmental Science, Qeshm Branch, Islamic Azad University, Qeshm, Iran, email: katayon\_hosseini@yahoo.com

<sup>d</sup>Department of Chemical Engineering, Faculty of Engineering, Khon Kaen University, Khon Kaen, Thailand, email: kitirote@kku.ac.th

<sup>e</sup>Department of Environmental Sciences, JSS Academy of Higher Education and Research, Sri Shivarathreeswara Nagara, Mysuru, Karnataka 570015, India, email: shivarajuenvi@gmail.com

<sup>f</sup>Wolfson Nanomaterials & Devices Laboratory, School of Computing, Electronics and Mathematics, Faculty of Science & Engineering, University of Plymouth, Devon, PL4 8AA, UK, email: D.F.Jenkins@plymouth.ac.uk

<sup>g</sup>Department of Environmental Health Engineering, Faculty of Health, Kurdistan University of Medical Sciences, Sanandaj, Iran, email: bshahmorady@gmail.com/bshahmoradi@muk.ac.ir

<sup>h</sup>Center for Solid Waste Research (CSWR), Institute for Environmental Research (IER), Tehran University of Medical Sciences, Tehran, Iran

Received 4 February 2023; Accepted 2 July 2023

---

### ABSTRACT

The presence of antibiotic drugs in the aquatic environment causes many health and environmental problems. The purpose of this study was to investigate the removal efficiency of erythromycin antibiotic from aqueous media using magnetic graphene oxide nanoparticles. Therefore, in the batch system, to assess the adsorption efficiency, the effect of different parameters such as pH (3–11), adsorbent dose (0.01–0.05 g), a contact time (10–120 min), initial concentration of erythromycin antibiotic (1–100 mg/L), and temperature (288–313 K) was evaluated. The results showed that the maximum amount of erythromycin adsorption occurred in conditions of pH = 3, the antibiotic concentration of 100 mg/L, contact time of 120 min, a temperature of 313 K, and an adsorbent dose of 0.01 g. Thermodynamic parameters showed that the adsorption process of erythromycin antibiotic in the temperature range of 288 to 313 K is spontaneous and endothermic. The coefficients of determination and adsorption rate constant calculated using the pseudo-second-order model were  $R^2 = 0.99$  and  $k_2 = 0.0004$ , respectively. The calculation based on the first-order model found  $R^2 = 0.2$  and  $k_1 = -0.0199$ ; it confirms that the pseudo-second-order model describes the laboratory data better than the first-order model. Meanwhile, the adsorption isotherms showed that antibiotic adsorption follows the Langmuir equation. According to the results of this research, a magnetic nanographene adsorbent with a high efficiency of 63.93% can be used to remove erythromycin from aqueous media.

*Keywords:* Antibiotic; Adsorption; Graphene oxide; Isotherms; Kinetics

---

\* Corresponding author.

## 1. Introduction

The rapid growth of human activities has led to the emergence of new toxic and dangerous chemical compounds called “emerging pollutants” that can cause unpredictable consequences for ecosystems [1]. Antibiotics, as one of the emerging pollutants, have received increasing attention in recent years [2]. Medicinal chemicals may be considered the main sources of antibiotic release in the environment through the discharge of wastewater from pharmaceutical industries, livestock hospitals, landfill leachates, and conventional wastewater treatment plants. The remarkable thing about the consumption of pharmaceuticals is that only less than 10% of them are transformed in the body, and the rest are eliminated from the human body without any change [3]. Conventional wastewater treatment plants have been designed regardless of removing antibiotics; hence, a significant amount of these chemicals are released into the aquatic media. The uncontrolled release of antibiotics in the environment causes the proliferation of antibiotic-resistant bacteria (ARB) and related antibiotic-resistant genes (ARG) in aquatic media. This brings about the ineffectiveness of antibiotics in the treatment of various diseases shortly [4]. Exposure to low doses of these emerging chemicals can affect non-target aquatic organisms and cause adverse physiological effects in humans [5]. Erythromycin ( $C_{36}H_{67}NO_{13}$ ) is a macrolide antibiotic that has prokinetic activity in low doses and can cross the blood-brain barrier. Macrolide antibiotics are one of the most prominent types of antimicrobial drugs [6]. Erythromycin has a strong antibacterial effect and, at the same time, causes water pollution, and its negative effect on water causes liver damage in humans [7]. Various chemical, physical, and biological methods have been considered for the removal of antibiotics, which are based on physical and chemical techniques and include oxidation, biological removal, reverse osmosis, coagulation, electrochemical treatment, removal of water hardness with lime, sedimentation, filtration, membrane filters, ion exchange, adsorption, and so on [8].

Adsorption is one of the principal methods, having some merits such as high adsorption capacity due to a high specific surface, absence of secondary toxic compounds, the possibility of adsorption of adsorbed pollutants, and reuse of adsorbents. The large specific surface and many active sites of nanoparticles enable them to have a higher adsorption capacity compared with micro-adsorbents and micro-particles [9].

Among different adsorbents, graphene and activated carbon are the most effective adsorbents [10]. The basis of these adsorbents is carbon, which, in terms of abundance, is not a concern for their preparation. Graphene oxide is the most common derivative of graphene, which is prepared during the reaction of graphite oxidation by the Hummers method [11]. Graphene oxide nanoparticles have special features such as high functionality, high adsorption capacity, easy synthesis, fast solubility in water, excellent biocompatibility, and low biological toxicity [12]. Graphene oxide is obtained from the complete oxidation and exfoliation of graphite, which includes a wide range of oxygen functional groups containing epoxy, hydroxyl, carbonyl, and carboxyl groups on its surface. These functional groups are

polar on the surface of graphene oxide and make it hydrophilic, which increases its solubility. In addition, magnetic graphene composite materials have been used to increase the affinity of other materials, promote phase separation, and increase adsorption efficiency. The magnetization of this material has been given more attention due to its high adsorption and easy separation from the environment, which can be easily controlled and cleaned by a simple magnetic process [13]. Iron oxide core is usually used in the manufacture of magnetic nanowires. This is due to the cheapness of iron oxide and the abundance of this metal in nature. Meanwhile, this metal is considered an environmentally safe metal [14].

Considering the increasing importance of water resource pollution, the use of high-efficiency processes in industries is significant and necessary. Therefore, this study was conducted to investigate the efficiency of the removal process of the erythromycin antibiotic using magnetic graphene oxide (MGO) nanoparticles from the aqueous medium.

## 2. Materials and methods

### 2.1. Synthesis of adsorbent

All the materials used were obtained from Merck, Germany. In this study, the synthesis of graphene nanostructures was carried out by the Hummers method [11]. In brief, first, 360 mL of sulfuric acid (96%), 40 mL of phosphoric acid (85%), and 4.0 g of graphite were mixed, and 18 g of potassium permanganate was gradually added to the mixture. When the reaction temperature reached about 288–313 K, the vessel was moved to an oil bath at a temperature of 50°C and stirred for 12 h, after which the vessel was taken out and allowed to remain at ambient temperature. Then, under the hood, the container was transferred into a flask containing 3.0 mL of hydrogen peroxide and 400 mL of ice water to separate the unreacted potassium permanganate. Using a centrifuge, the solids inside the container were separated and washed with 200 mL of double distilled water, and the solids were separated again using the centrifuge and washed twice with 200 mL of ethanol (96%) and 200 mL of 30% hydrochloric acid until all the metal ions and the used acids were separated [15]. The material obtained was washed with distilled water until reaching a pH of 7. Finally, the prepared graphene oxide was dried with the help of a freeze-dryer for 24 h. Graphene oxide was magnetized by the co-precipitation method. Thus, the resulting mixture was mixed in 500 mL of deionized distilled water and placed in an ultrasonic bath (40 kHz, 200 W) for 24 h. To the prepared mixture, 2.0 mM (540 mg) of hexavalent ferric chloride and 1.0 mM of tetravalent ferrous chloride (198 mg) were added while stirring using a mechanical stirrer. Then, 20 mL of 25% ammonia was slowly added to the suspension dropwise (about 30 min) in the presence of nitrogen gas at room temperature. After adding ammonia (25%), the temperature of the solution was increased to 80°C and refluxed for 5 h at that temperature in the presence of nitrogen gas. The product produced in this step was washed several times using double distilled water and ethanol until the pH of the washing water reached the neutral range, and finally, the adsorbent was dried using a freeze-dryer for 24 h [16].

## 2.2. Characterization of the adsorbent

Fourier-transform infrared (FTIR) spectra were taken to investigate the chemical structure and functional groups of the adsorbent. A field-emission scanning electron microscopy (FE-SEM) was used to investigate the morphology, appearance, particle shape determination, and particle size distribution. X-ray diffraction analysis was used to determine the crystalline structure of the adsorbent.

## 2.3. Preparation of the standard solution of the antibiotic

To prepare a stock solution, 100 mL of erythromycin antibiotic (purity of 89%) was added to distilled water. To ensure the complete dissolution of erythromycin, an ultrasonic bath was used. Then, by diluting the stock solution with double-distilled water, other solutions were prepared. Using 0.1 N NaOH or HCl, pH was adjusted using a pH meter (AZ8653 model, Taiwan). Each experiment was carried out inside a 100 mL Erlenmeyer flask containing 100 mL of different concentrations of antibiotic and adsorbent doses at different pH and contact times placed on a shaker (Parzan shaker model, Iran) for different periods (0–120 min). Then it was placed in a centrifuge (LASREVINU model, U.S.A.) at 4,000 rpm for 5 min. The residual concentration of erythromycin was determined using a spectrophotometer (UNIC UV-2100) at a wavelength of  $\lambda_{\max} = 285 \text{ nm}$  [17].

### 2.3.1. Calibration curve

To draw the calibration curve, the standard antibiotic solutions were prepared in the range of 1–150 mg/L using the stock solution. The absorbance of the prepared solutions from diluted to concentrated was read by a spectrophotometer using a quartz cell (Fig. 1).

## 2.4. Adsorption experiments

After preparing the standard solution for testing, each sample was placed on a shaker at a temperature of 298 K and a speed of 120 rpm. The effect of operational parameters was studied under different conditions. The parameters effective in adsorption studied were pH (3, 5, 7, 9, and 11), adsorbent dosage (0.01, 0.02, 0.03, 0.04, and 0.05 g), contact time (10, 30, 60, 90, and 120 min), initial concentration of erythromycin (1, 10, 25, 50, and 100 mg/L), and temperature

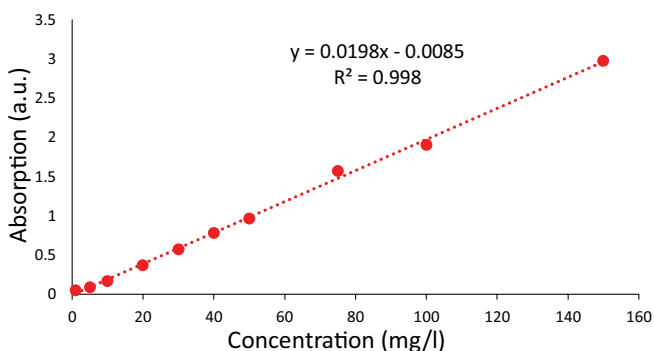


Fig. 1. Calibration curve of erythromycin.

(288, 293, 298, 303, 308, and 313 K). The removal efficiency of erythromycin antibiotic and adsorption capacity was calculated through Eqs. (1) and (2), respectively [17].

$$A\% = \frac{C_0 - C_e}{C_0} \times 100 \quad (1)$$

$$q_e = \frac{(C_0 - C_e)v}{m} \quad (2)$$

where  $A\%$  is adsorption efficiency (%),  $q_e$  represents the equilibrium adsorption capacity (mg/g),  $C_0$  is the initial concentration of erythromycin before adsorption (mg/L),  $C_e$  is the equilibrium concentration remaining in the solution in the equilibrium state after adsorption (mg/g),  $v$  is the volume of the solution (l), and  $m$  is the mass of the adsorbent (g).

### 2.4.1. Isotherm models

The adsorption isotherm expresses the equilibrium distribution of adsorption performance at different concentrations of adsorbent in a solution at a constant temperature. Isotherms are generally used to relate the amount of adsorbed ions to their equilibrium concentration in the solution [18]. To determine the optimal adsorption of erythromycin by MGO adsorbent, Langmuir and Freundlich models were used [19]. The Langmuir isotherm model is based on the single-layer, uniform, and homogeneous adsorption of the adsorbent with the same energy on all surfaces of the adsorbent, which is a linear equation [Eq. (3)]. Unlike the Langmuir model, the Freundlich isotherm is based on the multi-layered and heterogeneous adsorption of the adsorbed material on the adsorbent [20] and is in the form of Eq. (4).

$$\frac{C_0}{q_e} = \frac{1}{(q_{\max} b)} + \left( \frac{1}{q_{\max}} \right) C_e \quad (3)$$

where  $C_e$  is the equilibrium concentration of adsorbed ions (mg/L),  $q_{\max}$  is the maximum adsorption capacity (mg/g), and  $b$  is the Langmuir constant (mg/L) at a constant temperature.

$$\ln q_e = \ln K_f + \frac{1}{n} \ln C_e \quad (4)$$

where  $q_e$  is the number of ions adsorbed (mg/g),  $C_e$  is the equilibrium concentration of adsorbed ions (mg/L), and  $K_f$  is the Freundlich constant. The value of  $n$  in the Freundlich equation shows the degree of non-linearity between the concentration of the solution and the adsorption process. If the value is  $n = 1$ , it is linear adsorption, if  $n > 1$ , adsorption is a chemical process, and if  $n < 1$ , adsorption is a physical process [21].

### 2.4.2. Kinetic models

Adsorption kinetics is a multi-stage process that includes the transfer of adsorbed molecules from the

soluble phase to the surface of the adsorbent and then the penetration of soluble particles into the internal pores. To provide information about the factors affecting the reaction rate, it is necessary to study the kinetics. Kinetics determines the amount of antibiotic adsorption at the optimal time and is one of the important features to determine the adsorption efficiency [22]. For this purpose, we used the pseudo-first-order kinetic model [Eq. (5)] and the pseudo-second-order kinetic model [Eq. (6)].

$$\ln(q_e - q_t) = \ln q_e - k_1 t \quad (5)$$

$$\frac{t}{q} = \frac{t}{q_e} + \frac{1}{K_2 q_e} \quad (6)$$

where  $q_e$  is the amount of adsorbed metal ions per adsorbent at the time of equilibrium (mg/g).  $q_t$  is the amount of adsorbed ions per adsorbent material at time  $t$  and  $k_1$  is the adsorption rate constant.  $k_2$  is the adsorption rate constant for the pseudo-second-order kinetic model (g/mg·min).

#### 2.4.3. Thermodynamic models

The study of adsorption thermodynamics is necessary to monitor the energy changes during the adsorption process. To study the enthalpy and entropy parameters, are obtained by using the Van't Hoff matching diagram by plotting the  $\ln K$  vs.  $1/T$  curve. Thermodynamic parameters such as Gibbs free energy changes ( $\Delta G^\circ$ ) (mol/J), standard enthalpy changes ( $\Delta H^\circ$ ), and standard entropy changes ( $\Delta S^\circ$ ) were calculated using Eqs. (7) and (8), respectively [23]. Enthalpy changes indicate changes in the internal energy level of the solution during the adsorption process, based on which it is possible to determine whether the process is exothermic ( $\Delta H^\circ < 0$ ) or endothermic ( $0 > \Delta H^\circ$ ) [18]. The coefficient of determination ( $R^2$ ) was used to evaluate the models. The closer this value is to 1, the better the fit of the desired model.

$$\Delta G^\circ = -RT \ln K_c \quad (7)$$

$$\Delta G^\circ = \Delta H^\circ - T\Delta S^\circ \quad (8)$$

where  $\Delta G^\circ$  is the standard free energy change,  $R$  is the global gas constant = 8.314 kJ/mol,  $T$  is the absolute temperature (K), and  $K_c$  is the distribution coefficient.  $K_c$  is calculated by dividing the concentration in liquid phase ([solute]<sub>liquid</sub>) by the concentration in the solid phase ([solute]<sub>solid</sub>) [24].

## 3. Results and discussion

### 3.1. Characterization results of the adsorbent

#### 3.1.1. Fourier-transform infrared spectroscopy

FTIR spectra were taken of MGO nanoparticles before and after the adsorption of erythromycin. As shown in Fig. 2, functional groups of amino, carbonyl, C=C, and C=N double bond, as well as the nitrile triple bonds and the single bond of C–O, are distinguishable. As can be seen in the

spectrum, the peak in 2,000  $\text{cm}^{-1}$  corresponds to the stretching frequency of the O=C group, the 2,300  $\text{cm}^{-1}$  peak corresponds to the C=N group, and the 1,600  $\text{cm}^{-1}$  spectrum corresponds to the C=C group, which indicates good adsorbent conditions for adsorbing the erythromycin antibiotic [12].

#### 3.1.2. Field-emission scanning electron microscopy

FE-SEM was used to observe the morphology and physical shape of the surface of prepared MGO nanoparticles. The voids in Fig. 3 show before and after adsorption, which represents empty sites that can adsorb erythromycin. Due to the special surface of MGO nanoparticles, voids can be seen in their particles after adsorption, which means that the adsorbent can be used several times in the continuous adsorption system without decreasing the adsorption efficiency [12].

#### 3.1.3. X-ray diffraction

Strong peaks at  $2\theta$  of 27.92°, 29.32°, and 26.48° were observed, and these peaks indicate the high degree of crystallinity of the nanoparticles due to internal and intermolecular hydrogen bonds. In general, it indicates the crystalline and non-crystalline structures of the adsorbent (Fig. 4).

### 3.2. Effect of influencing parameters on the adsorption of erythromycin

#### 3.2.1. Effect of pH

The effect of pH is considered one of the most crucial parameters to investigate the adsorption process [25]. Fig. 5 shows the effect of pH on the adsorption of erythromycin. To determine the effect of erythromycin adsorption efficiency using MGO nanoparticles, the rest of the parameters were kept constant, and different pHs between 3 and 11 were considered with a fixed antibiotic solution volume of 100 mL. The results showed that the amount of antibiotic adsorption on the adsorbent used is strongly influenced by the pH of the solution. In acidic pHs up to 5, the removal efficiency of antibiotics was high, while at pH 6 and higher, a sharp reduction followed by almost constant efficiency is

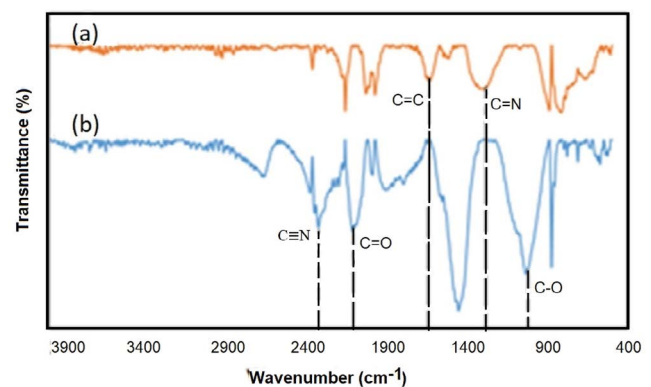


Fig. 2. Fourier-transform infrared spectra of magnetic graphene oxide nanoparticles: (a) before and (b) after adsorption of erythromycin.

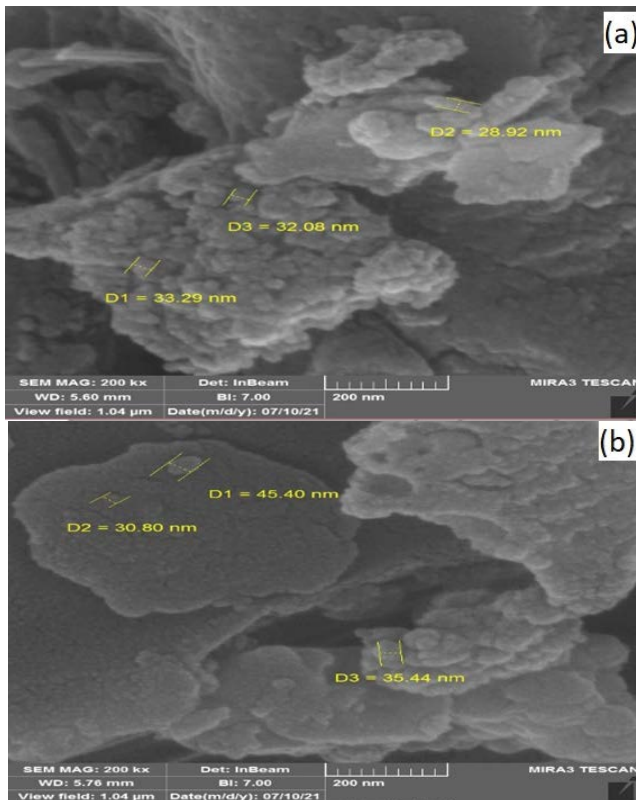


Fig. 3. Field-emission scanning electron microscopy images of magnetic graphene oxide nanoparticles: (a) before and (b) after adsorption of erythromycin.

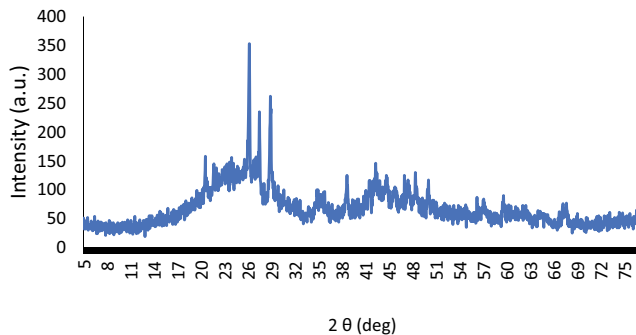


Fig. 4. X-ray diffraction pattern of magnetic graphene oxide nanoparticles.

noticeable. The reason for the high adsorption efficiency at acidic pH is that the active sites on the surface of the adsorbent are protonated, and the charge density on the surface of the adsorbent increases. The reason for the increase in positive charge can be expressed as the point where the positive and negative charges of  $pH_{zpc}$  are equal to each other, which is called the isoelectric point of the adsorbent ( $pH_{zpc}$ ). Above  $pH_{zpc}$ , the charge potential is negative, below  $pH_{zpc}$ , the charge potential is negative, and below  $pH_{zpc}$ , the charge potential on the adsorbent is positive. Considering that  $pH_{zpc}$  was 5 in this research, as a result, at pH higher than 5, the adsorbent surface has a negative charge, and at

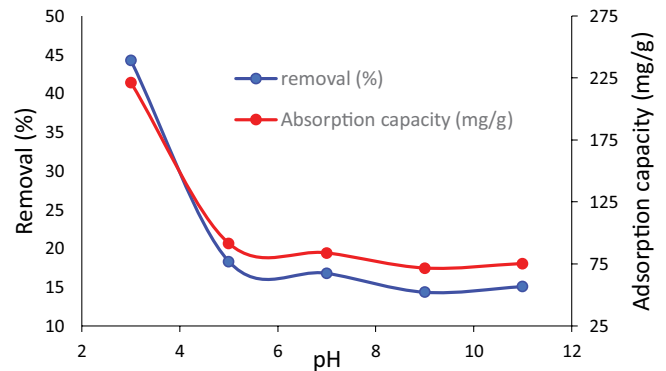


Fig. 5. Effect of pH changes on the adsorption efficiency and capacity of erythromycin.

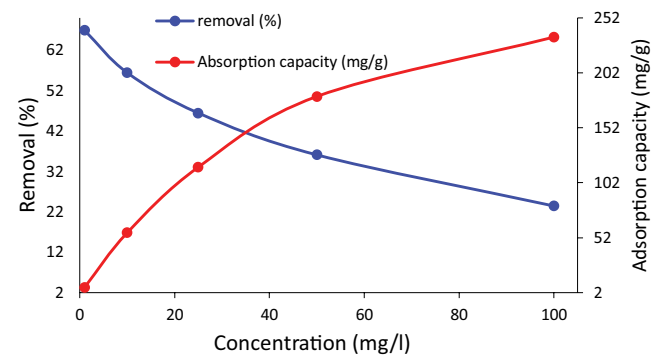


Fig. 6. Effect of changes in the concentration of antibiotic on its removal efficiency and adsorption capacity of erythromycin.

pH less than 5, the charge potential on the adsorbent surface is positive. Therefore, at a pH less than 5, the anions of antibiotics will be adsorbed by the positive charges generated on the adsorbent due to electrostatic forces [26]. According to Fig. 5, it can be seen that the removal rate of erythromycin increased from 15% at pH 11 to 44% at pH 3, and the optimal pH 3 was considered for the antibiotic, in this range, the equilibrium adsorption capacity and removal percentage of erythromycin were 221 mg/g (44%).

In the erythromycin antibiotic, the large decrease in adsorption capacity at pH = 3 is due to the ionization of the solution at high pH. Finally, due to the area of the negative charge of the adsorbent, the possibility of connecting the adsorbent and the adsorbed material is lost, and the amount of adsorption capacity is greatly reduced.

### 3.2.2. Effect of erythromycin concentration

The result of the effects of the initial concentration of erythromycin solution on the adsorption capacity and removal percentage can be seen in Fig. 6. Based on Fig. 6, the adsorption capacity increased with the increase in concentration. For the adsorption of erythromycin antibiotic, the highest erythromycin adsorption capacity of 234.51 mg/g was obtained at a concentration of 100 mg/L.

The results showed that the adsorption of the antibiotic decreases with increasing concentration, but the adsorption

capacity increases and has an upward trend. It could be attributed to the possibility of increased collision and contact between the adsorbent and the adsorbed material. The multiplicity of treatment molecules and the constant number of adsorption sites can be another factor [26].

### 3.2.3. Effect of adsorbent dosage

The result of the effects of the amount of adsorbent on the removal percentage and the adsorption capacity of erythromycin is depicted in Fig. 7. The removal percentage for erythromycin increased from 34.36 to 58.71%, and the equilibrium adsorption capacity decreased from 181.72 to 58.71 mg with the increasing amount of adsorbent. The results showed that the efficiency increased with the increase in the amount of adsorbent dose, which is due to the increase in the area of the adsorbent or the easier accessibility of erythromycin molecules to the pores of MGO nanoparticles because, with the increase in the adsorbent amount, the contact surface of the adsorbent increases and achieves more access to the adsorption sites by antibiotic molecules, and leading to an increase in the adsorption of this substance. By increasing the adsorbent dose, more surface area or more adsorption sites are prepared for a constant concentration of antibiotics until optimal efficiency, but after the optimal performance, the increasing adsorbent doses had no effect on the amount of antibiotic removal but had a negative effect on the adsorption capacity. It is probably because the active sites of the adsorbent are not occupied during the adsorption process [27]. According to the results obtained, the adsorbent dose of 0.01 was considered the optimal dose.

### 3.2.4. Effect of time

Contact time is an important factor for rapid adsorption and the effective use of biosorbents. The highest adsorption percentage (47.72) and adsorption capacity (189.85) occurred in 120 min. Fig. 8 shows that as the contact time increases, the percentage of removal increases, so that the removal rate of the antibiotic was very high for the first 60 min, and then the process of increasing the removal efficiency continued at a slower rate until 60 min, the equilibrium was reached in 60 min. This shows that MGO nanoparticles have

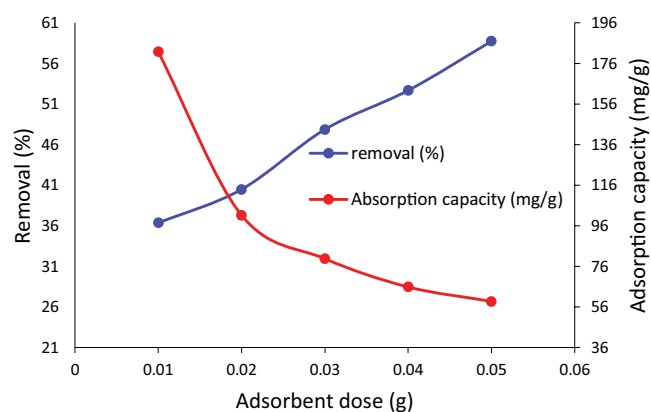


Fig. 7. Effect of adsorbent dosage on the antibiotic removal and adsorption capacity of erythromycin.

high efficiency in antibiotic removal in a short time, and in the early stages, the active sites involved in the adsorption process are quickly saturated [28].

### 3.2.5. Effect of temperature

According to Fig. 9, it was found that the removal percentage of erythromycin decreased with the increase in temperature, and the highest removal percentage was achieved at 288 K. It was found that the adsorption of erythromycin by MGO nanoparticles increased with increasing temperature, from 288 to 313 K. Table 1 shows that the reaction is spontaneous because the values of the free energy of the process are negative at all the studied temperatures and change with increasing temperature. The positive value of  $\Delta H^\circ$  indicates the endothermic nature of the adsorption process, and the positive value of  $\Delta S^\circ$  indicates the affinity of the adsorbent to the adsorbed substance in the solution and some structural changes in the adsorbent and the adsorbed antibiotic with increasing temperature, the values of  $\Delta G^\circ$  decreased. This means that increasing the temperature tends to increase the adsorption capacity of erythromycin [24]. Fig. 9 shows that the antibiotic removal percentage decreases with increasing temperature. The highest target percentage and adsorption capacity for erythromycin are 25.52 and 62.44, respectively.

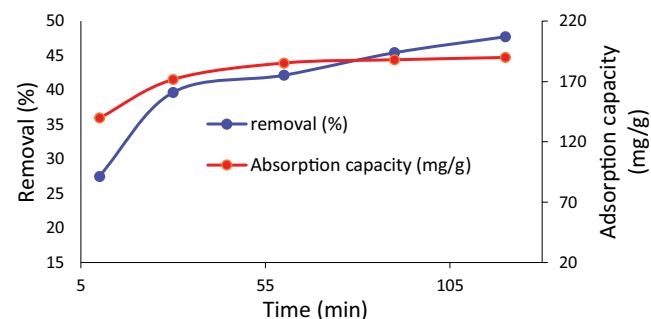


Fig. 8. Effect of contact time on the antibiotic removal and adsorption capacity of erythromycin.

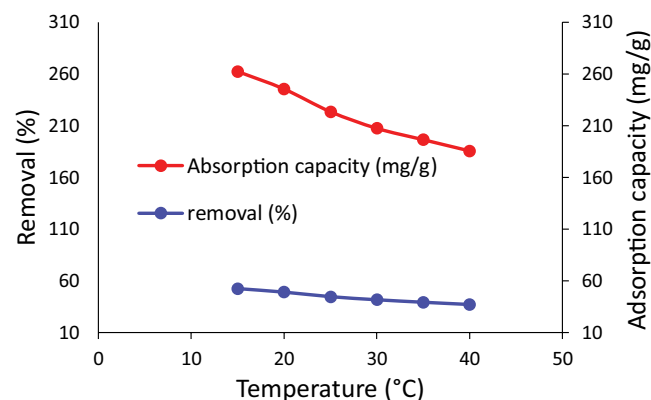


Fig. 9. Effect of temperature on the antibiotic removal and adsorption capacity of erythromycin.

Table 1  
Thermodynamic parameters (kJ/mol) of erythromycin adsorption

T (K)	$\Delta G^\circ$	$\Delta H^\circ$	$\Delta S^\circ$
288	-5,751/55,306		
293	-5,521/227,589		
298	-5,179/056,225		
303	-4,934/070,218	0.0033256	0.0199536
308	-4,782/579,036		
313	-4,620/842,923		

### 3.3. Adsorption isotherms

Adsorption isotherms are equilibrium data used to describe the binding behavior between the treatment and the adsorbent. Isotherms express the adsorption capacity of an adsorbent. In this study, Langmuir and Freundlich's isotherms were used to analyze the experimental data and interpret the equilibrium state in adsorption between treatment and liquid. According to Table 2 and Fig. 10, the Langmuir model ( $R^2 = 0.99$ ) can better describe the adsorption of erythromycin ions compared with the Freundlich ( $R^2 = 0.97$ ) model. In addition, considering the obtained  $b$  (1,497.17), it confirms the fit of Langmuir. Since the Langmuir model refers to the homogeneity of the adsorbent surfaces, it can be concluded that the adsorption of erythromycin by MGO nanoparticles was performed in a single layer. According to the adsorption capacity calculated, the adsorption capacity of the adsorbent used in this research was compared with the performance of different adsorbents in removing erythromycin solution (Table 2). A comparison of the maximum adsorption capacity of MGO nanoparticles with other natural adsorbents shows the high efficiency of this adsorbent. The value of  $q_{\max}$  in the Langmuir model for erythromycin was 285.71, which proves that magnetic graphene oxide nanoparticles can adsorb more antibiotic molecules compared with the equilibrium state. The dimensionless  $R_L$  for erythromycin was in the range of 0–1, which indicates the optimal adsorption efficiency.

The study of adsorption kinetics provides important information in the fields of reaction pathways and adsorption speed. Kinetics determines the adsorption rate of the adsorbent at the optimal time and is one of the important characteristics to determine the efficiency of the adsorbent [29]. Adsorption kinetics control the solubility at the solid–liquid interface [30]. In this study, two kinetic models, pseudo-first-order and pseudo-second-order, were used to determine the mechanism of antibiotic adsorption using MGO nanoparticles. For the kinetics of antibiotic adsorption, the adsorption test was performed under optimum conditions (pH = 3, adsorbent dose = 0.01, and erythromycin concentrations = 50 mg/L). Fig. 11 shows the adsorption kinetics of erythromycin.

Considering that sometimes several equations can describe kinetic data, the best equation is selected based on the highest coefficient of determination ( $R^2$ ). This factor is a necessary condition for choosing the best model. But it is not a sufficient condition. The equation that has the highest

Table 2  
Parameters of isotherm models for erythromycin adsorption

Model	$K_f$	$b$ (L/mg)	$q_{\max}$ (mg/g)	$R^2$	$R_L$	$n$
Freundlich	1.964	–		0.9783		0.3541
Langmuir	–	17.1497	16.666	0.9939	0.0011	

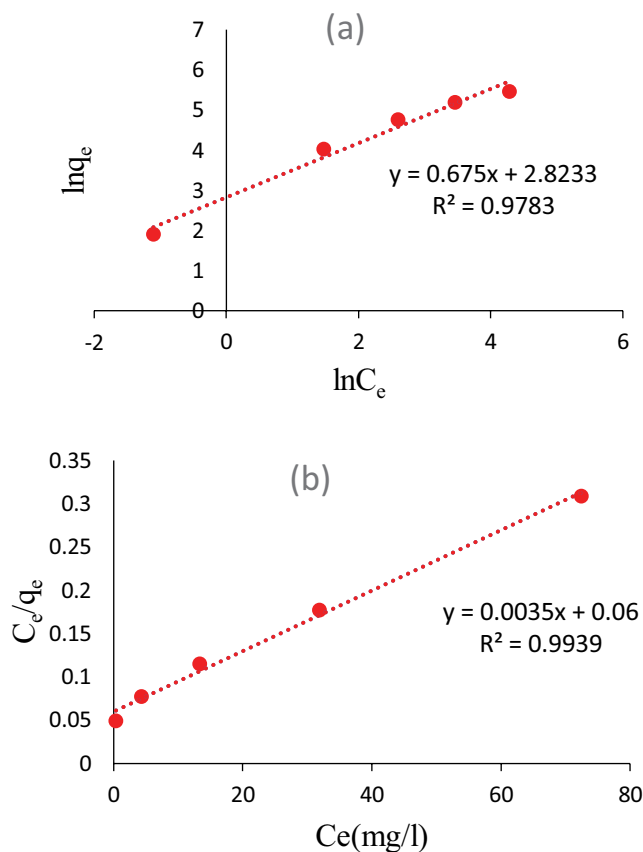


Fig. 10. Adsorption isotherms for erythromycin: (a) Langmuir and (b) Freundlich.

$R^2$  and the lowest standard error of estimation is known as the best equation for justifying the removal of erythromycin. As shown in Fig. 11, the pseudo-second-order model with a higher  $R^2 = 0.99$  describes the test data better compared with the pseudo-first-order model ( $R^2 = 0.20$ ) and shows that chemical adsorption controls the surface adsorption process [31]. Nevertheless, the results showed that the pseudo-second-order model in estimating the  $q_e$  value (256.41 mg/g) is more successful compared with the pseudo-first-order model ( $q_e = 15.94$  mg/g). By increasing the contact time and increasing the opportunity for erythromycin ions to collide with the adsorbent, the percentage of adsorption increases. Within 60 min after the contact between MGO nanoparticles and the erythromycin solution, the adsorption process reaches equilibrium. Increasing the contact time after this time does not affect the percentage of adsorption.

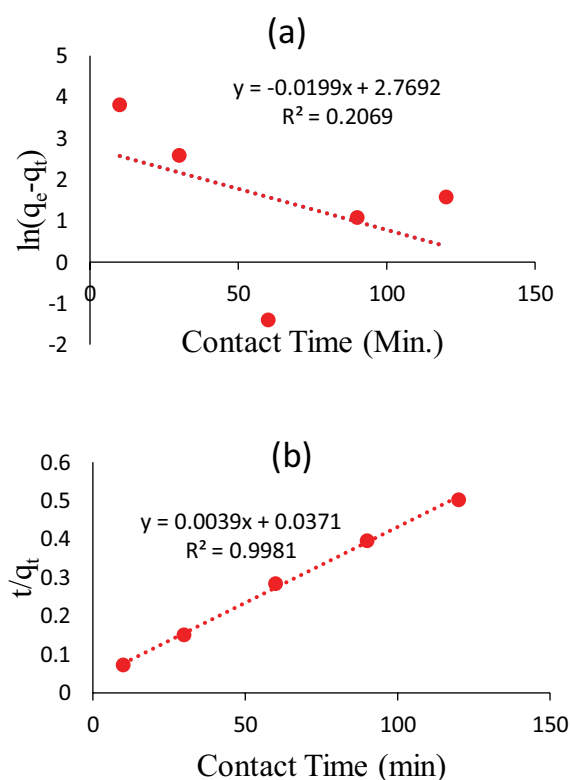


Fig. 11. Kinetics models for erythromycin adsorption: (a) pseudo-first-order and (b) pseudo-second-order.

### 3.4. Adsorption thermodynamics

To study the effect of temperature (288–313 K) on the adsorption of erythromycin by MGO nanoparticles, the adsorption experiments were carried out under the same conditions as described in 3.3. The enthalpy and entropy parameters were evaluated using the Van't Hoff equation ( $\ln K_c$  vs.  $1/T$ ). Fig. 12 shows the Van't Hoff diagram for antibiotic adsorption using a magnetic oxide nanographene adsorbent. The positive slope of the Van't Hoff curve indicates the exothermicity of the erythromycin adsorption. On the other hand, with the increase in temperature, the adsorption capacity decreases, and as a result, the amount of  $K_c$  decreases. Thermodynamic properties such as the change in  $\Delta G^\circ$ ,  $\Delta H^\circ$ , and  $\Delta S^\circ$  for the adsorption process of the antibiotic on synthesized MGO nanoparticles were fully investigated. The calculated thermodynamic variables at temperatures of 288, 293, 298, 303, 308, and 313 K, and the correlation coefficient are given in Table 1. According to Table 1, the values of  $\Delta G^\circ$  are negative, which indicates that the adsorption of erythromycin is acceptable and spontaneous. Moreover, the decrease of negative values of  $\Delta G^\circ$  with increasing temperature indicates that with increasing temperature, the tendency of erythromycin molecules towards the magnetic graphene oxide nanoparticles and the connection of the molecules with the surface of the magnetic graphene oxide nanoparticles decrease, so the adsorption decreases. The negative values of enthalpy changes ( $\Delta H^\circ$ ) indicate the exothermicity of adsorption. The negative values of  $\Delta S^\circ$  also indicate the decrease of

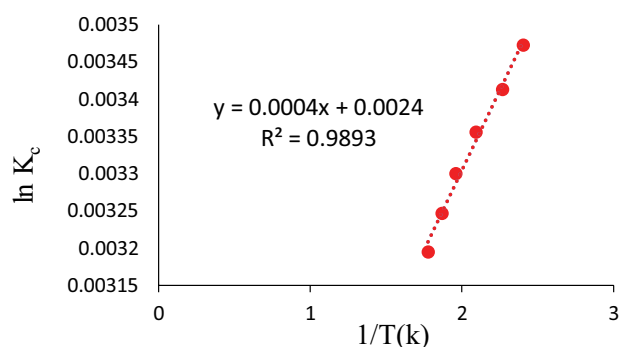


Fig. 12. Van't Hoff diagram of erythromycin adsorption using magnetic graphene oxide nanoparticles.

disorder with increasing temperature in the common phase of solid and liquid during the adsorption process.

### 4. Conclusion

In this study, it was observed that the investigated parameters (pH, adsorbent amount, contact time, temperature, and initial concentration) have a significant effect on the adsorption process. The Langmuir model was more consistent with the experimental data. Moreover, it was found that pseudo-second-order kinetics controls the speed of the process, the surface adsorption process of erythromycin is a chemical process, and the adsorption rate of erythromycin decreases with increasing temperature. The obtained thermodynamic parameters showed that the erythromycin adsorption process is spontaneous, the enthalpy and entropy changes are positive, and the spontaneity of the erythromycin ion adsorption process is because of the entropy changes. This factor causes the process to take place better at a higher temperature. It should be noted that the maximum adsorption was achieved under conditions of pH = 3, contact time = 60 min, ambient temperature = 298 K, adsorbent mass = 0.01 g, and antibiotic concentration = 100 mg/L. The results of this research showed that MGO nanoparticles can be used as a potential bio-adsorbent to remove erythromycin from wastewater, which has the advantages of availability, cost-effectiveness, and high performance.

### References

- [1] I. Anastopoulos, I. Pashalidis, A.G. Orfanos, I.D. Manariotis, T. Tatarchuk, L. Sellaoui, A. Bonilla-Petriciolet, A. Mittal, A. Núñez-Delgado, Removal of caffeine, nicotine and amoxicillin from (waste)waters by various adsorbents: a review, *J. Environ. Manage.*, 261 (2020) 110236, doi: 10.1016/j.jenvman.2020.110236.
- [2] S. Zhi, S. Shen, J. Zhou, G. Ding, K. Zhang, Systematic analysis of occurrence, density and ecological risks of 45 veterinary antibiotics: focused on family livestock farms in Erhai Lake basin, Yunnan, China, *Environ. Pollut.*, 267 (2020) 115539, doi: 10.1016/j.envpol.2020.115539.
- [3] A. Osińska, E. Korzeniewska, M. Harnisz, E. Felis, S. Bajkacz, P. Jachimowicz, S. Niestępski, I. Konopka, Small-scale wastewater treatment plants as a source of the dissemination of antibiotic resistance genes in the aquatic environment, *J. Hazard. Mater.*, 381 (2020) 121221, doi: 10.1016/j.jhazmat.2019.121221.
- [4] G. Bairán, G. Rebollar-Pérez, E. Chávez-Bravo, E. Torres, Treatment processes for microbial resistance mitigation: the

- technological contribution to tackle the problem of antibiotic resistance, *Int. J. Environ. Res. Public Health*, 17 (2020) 8866, doi: 10.3390/ijerph17238866.
- [5] H. Schwartz, L. Marushka, H.M. Chan, M. Batal, T. Sadik, A. Ing, K. Fediuk, C. Tikhonov, Pharmaceuticals in source waters of 95 first nations in Canada, *Can. J. Public Health*, 112 (2021) 133–153.
- [6] P. Fathollahi, H. Rezaei, M. Sadeghi, S. Namroodi, Removal of Erythromycin Antibiotic with Modified Magnetic Oxide Nanographene From Aqueous Medium (Adsorption Kinetics), The First National Conference of Community-Oriented Researches in Agriculture, Natural Resources and Environment, Hamedan, Iran, 2021 (in Persian).
- [7] J. Peng, Q. Huang, W. Zhuge, Y. Liu, C. Zhang, W. Yang, G. Xiang, Blue-light photoelectrochemical sensor based on nickel tetra-aminated phthalocyanine-graphene oxide covalent compound for ultrasensitive detection of erythromycin, *Biosens. Bioelectron.*, 106 (2018) 212–218.
- [8] P. Fathollahi, H. Rezaei, M. Sadeghi, S. Namroodi, Removal of cadmium ion from aqueous solutions using magnetic graphene oxide nanoparticles, *Environ. Water Eng.*, 8 (2022) 856–873.
- [9] N. Hamidianfar, M.H. Abolhasani, M. Ataabadi, Investigation of the effect of using iron oxide nanoparticles in removing cadmium from aqueous media: a laboratory study, *J. Rafsanjan Univ. Med. Sci.*, 18 (2020) 1253–1269 (in Persian).
- [10] Y. Liu, W. Fan, Z. Xu, W. Peng, S. Luo, Comparative effects of graphene and graphene oxide on copper toxicity to *Daphnia magna*: role of surface oxygenic functional groups, *Environ. Pollut.*, 236 (2018) 962–970.
- [11] H. Yu, B. Zhang, C. Bulin, R. Li, R. Xing, High-efficient synthesis of graphene oxide based on improved Hummers method, *Sci. Rep.*, 6 (2016) 36143, doi: 10.1038/srep36143.
- [12] N. Rouniasi, S.M. Monavari, M.A. Abdoli, M. Baghdadi, A. Karbasi, Removal of heavy metals of cadmium and lead from aqueous solutions using graphene oxide nanosheets process optimization by response surface methodology, *Iran. J. Health Environ.*, 11 (2018) 197–214 (in Persian).
- [13] M.A. Renu, K. Singh, Heavy metal removal from wastewater using various adsorbents: a review, *J. Water Reuse Desal.*, 7 (2017) 387–419.
- [14] A. Khoshnoodfar, N. Bahramifar, H. Younesi, Synthesis and application of magnetic graphene nanocomposite for removal sodium dodecyl benzenesulfonate (SDBS) from aqueous solutions, *J. Nat. Environ.*, 72 (2019) 325–338.
- [15] M. Gharebiglou, I. Mir Shahabeddin, H. Erfan-Niya, A.A. Entezami, Improving the mechanical and thermal properties of chemically modified graphene oxide/polypropylene nanocomposite, *Modares Mech. Eng.*, 16 (2016) 196–206 (in Persian).
- [16] D.R. Dreyer, S. Park, C.W. Bielawski, R.S. Ruoff, The chemistry of graphene oxide, *Chem. Soc. Rev.*, 39 (2010) 228–240.
- [17] F. Bahmei, N. Bahramifar, H. Younesi, V. Tolstoy, Synthesis of porous graphene nanocomposite and its excellent adsorption behavior for Erythromycin antibiotic, *Nanosyst. Phys. Chem. Math.*, 11 (2020) 214–222.
- [18] S.H. Gupta, A. Kumar, Removal of nickel(II) from aqueous solution by biosorption on *A. barbadensis* Müller waste leaves powder, *Appl. Water Sci.*, 12 (2019) 27–36.
- [19] E. Mohammadnia, M. Hadavifar, H. Veisi, Kinetics and thermodynamics of mercury adsorption onto thiolated graphene oxide nanoparticles, *Polyhedron*, 173 (2019) 114139, doi: 10.1016/j.poly.2019.114139.
- [20] N. Ayawei, A.N. Ebelegi, D. Wankasi, Modelling and interpretation of adsorption isotherms, *J. Chem.*, 2017 (2017) 3039817, doi: 10.1155/2017/3039817.
- [21] S.A. Olawale, A. Wosilat Funke, A. Haruna Dede, A. Habeeb, Isotherm studies of the biosorption of Pb(II) and Cu(II) using chicken feather, *Asia. J. Adv. Res. Rep.*, 1 (2018) 1–9.
- [22] J.L. Wang, C. Chen, Biosorption of heavy metals by *Saccharomyces cerevisiae*: a review, *Biotechnol. Adv.*, 24 (2006) 427–51.
- [23] R. Li, Z. Wang, X. Zhao, X. Li, X. Xie, Magnetic biochar-based manganese oxide composite for enhanced fluoroquinolone antibiotic removal from water, *Environ. Sci. Pollut. Res.*, 25 (2018) 31136–31148.
- [24] H.N. Tran, Improper estimation of thermodynamic parameters in adsorption studies with distribution coefficient  $K_d$  ( $q/C_e$ ) or Freundlich constant ( $K_f$ ): considerations from the derivation of dimensionless thermodynamic equilibrium constant and suggestions, *Adsorpt. Sci. Technol.*, 2022 (2022) 5553212, doi: 10.1155/2022/5553212.
- [25] Y. Zhang, W.T. Frankenberger, Factors affecting removal of selenate in agricultural drainage water utilizing rice straw, *Sci. Total Environ.*, 305 (2003) 207–216.
- [26] D. Balarak, F. Kord Mostafapour, A. Rakhsh Khorshid, Isotherm and kinetic study on the adsorption of penicillin G from aqueous solution by using modified canola, *J. Rafsanjan Univ. Med. Sci.*, 15 (2016) 101–114.
- [27] B. Kakavandi, R. Rezaei Kalantary, A. Jonidi Jafari, A. Esrafiy, A. Gholizadeh, A. Azari, Efficiency of powder activated carbon magnetized by  $Fe_3O_4$  nanoparticles for amoxicillin removal from aqueous solutions: equilibrium and kinetic studies of adsorption process, *Iran. J. Health Environ.*, 7 (2014) 21–34 (in Persian).
- [28] A.A. Babaei, K. Ahmadi, I. Kazeminezhad, S.N. Alavi, A. Takdastan, Synthesis and application of magnetic hydroxyapatite for removal of tetracycline from aqueous solutions, *J. Mazandaran Univ. Med. Sci.*, 26 (2016) 146–159.
- [29] X.S. Wang, J.J. Ren, H.J. Lu, L. Zhu, F. Liu, Q.Q. Zhang, J. Xie, Removal of Ni(II) from aqueous solutions by nanoscale magnetite, *Clean Soil Air Water*, 38 (2010) 1131–1136.
- [30] K.S. Low, C.K. Lee, S.C. Liew, Sorption of cadmium and lead from aqueous solutions by spent grain, *Process Biochem.*, 36 (2000) 59–64.
- [31] P. Chingombe, B. Saha, R.J. Wakeman, Sorption of atrazine on conventional and surface modified activated carbons, *J. Colloid Interface Sci.*, 302 (2006) 408–416.